International Journal of the Korean Society of Precision Engineering Vol. 4, No. 2, March 2003.

Theoretical Verification on the Motion Error Analysis Method of Hydrostatic Bearing Tables Using a Transfer Function

Chun Hong Park[1], Yoon Jin Oh[1], Chan Hong Lee[1] and Joon Hee Hong[2]

[1] Machine tools group, Korea Institute of Machinery & Materials, Daejeon, South Korea
[2] Department of mechanical engineering, Chungnam University, Daejeon, South Korea

ABSTRACT

A new method using a transfer function is introduced in the present paper for analyzing the motion errors of hydrostatic bearing tables. The relationship between film reaction force in a single-side hydrostatic pad and the form error of guide rail is derived at various spatial frequencies by finite element analysis, and it is expressed as a transfer function. This transfer function clarifies so called 'the averaging effect of an oil film' quantitively. It is found that the amplitude of film force is reduced as the spatial frequency increases or the relative width of the pocket is reduced. The motion errors of a multi pad type table are estimated using a transfer function, the form errors of a guide rail and the geometric relationship between the pads. The method is named as the Transfer Function Method (TFM). The motion errors calculated by the TFM show good agreement with the motion errors calculated by the Multi Pad Method considering the entire table as an analysis object. From the results, it is confirmed that the proposed TFM is very effective to analyze the motion errors of hydrostatic tables.

Keywords : Hydrostatic bearing table, Motion error, Transfer function, Finite element analysis

1. Introduction

The linear and angular motion error of a hydrostatic table can be analyzed by the finite element method with finely divided meshes on the entire table, and the method is named as the MPM(Multi Pad Method)[1,2]. But the method has a disadvantage that the calculating time is abruptly increased as the number of mesh is increased for evaluating the influence of high spatial frequencies. Also, when the size of bearing or the rail form error is changed, the calculation should be repeated again from the mesh generation process.

In this paper, a transfer function is defined as the magnitude of film force in a pad corresponding to the spatial frequencies of rail form error, and a new method using the transfer function is proposed for analyzing the motion errors of hydrostatic tables. By this method, modeling of motion in a multi pad type table is simplified as the geometrically superposed motion of a pad with spatial phase shift.

The calculation error caused by the sinusoidal approximation of film force is estimated, and the relationship between the transfer function and the averaging effect of an oil film is discussed. Finally, for evaluating the effectiveness of the TFM, the analyzed motion errors are compared with the analyzed results by the MPM in the case of a single-side and a double-sides table respectively.

2. Modeling of a Hydrostatic Table

Fig. 1 shows the static equilibrium model of force in a single-side hydrostatic table. The elastic deformation of table body is neglected. Therefore, the variation of film force in each pad is transformed to the vertical displacement of the pad. In the figure, m is the number of pad, Xci is the distance between the center of table and the center of each pad, L is the length of rail, $Fi(x)$ and $zi(x)$ are the film force and the vertical displacement of i^{th}

pad when the coordinate of table center is x, and $\theta(x)$ is the inclined angle of table.

As shown in the figure, each pad of a table passes the same position on the rail successively with constant geometric interval. The hydrostatic tables generally consist of multiple number of pad, and each pad is designed with the same dimension. Therefore, if the relationship between a pad and a rail is known, the motion errors of table can be analyzed from the geometrical relationship between the pads.

Considering the equilibrium state of force including the influence of rail form error $e(x)$ in i^{th} pad, the pad has vertical displacement $z_i(x)$ by the variation of film force $f_{ei}(x)$ corresponding to the rail form error $e(x)$, and the film force of i^{th} pad becomes $F_i(x)$. Assuming that the film stiffness K_0 is constant within the range of vertical displacement, the relationship between the film force and the vertical displacement of each pad is described as follows;

$$f_i(x) = f_{ei}(x) - K_0 z_i(x) \tag{1}$$

Using the relation of Eq.(1), the equilibrium conditions of force and moment are represented as Eq.(2) and (3).

$$\sum_{i=1}^{m} \{f_{ei}(x) - K_0 z_i(x)\} = 0 \tag{2}$$

$$\sum_{i=1}^{m} \{f_{ei}(x) - K_0 z_i(x)\}\left(X_{ci} + \frac{ml}{2}\right) = 0 \tag{3}$$

$$\frac{ml}{2} \le x \le L - \frac{ml}{2}$$

On the other hand, Assuming that it is periodic function, the rail form error is represented as follows;

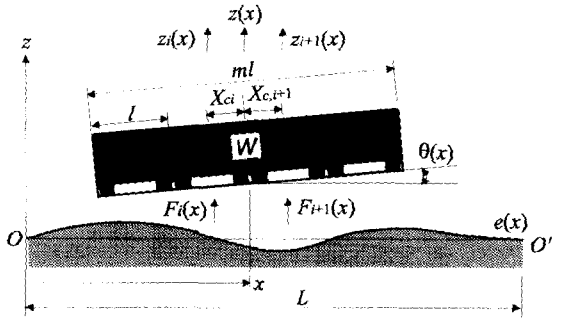

Fig. 1 Static equilibrium model of a single pad type hydrostatic table in the transfer function method

$$e(x) = a_0 + \sum_{k=1}^{n}\left(a_k \cos\frac{2k\pi}{L}x + b_k \sin\frac{2k\pi}{L}x\right) \tag{4}$$

Now, for the effectiveness of the motion error analysis, a transfer function is introduced. It is defined as the ratio of the varying film force to the magnitude of spatial frequencies of rail form error. The transfer function can be calculated theoretically using the dimensions of a designed table.

Using the calculated transfer function, the measured rail form error and the relationship of Eq.(2)~(4), the geometric attitude of a table in the equilibrium state can be calculated. In this case, the angular displacement can be calculated by Eq.(5) under assumption that it takes place only by the difference of film force between the pads.

$$\theta(x) = \{z_m(x) - z_1(x)\}/(m-1)l \tag{5}$$

The motion errors of a table are obtained by the iterative calculation on the attitude of a table over the full moving stroke.

3. The Transfer Function Method

3.1 The transfer function and the film force

For acquiring a transfer function, the case in which a pad moves on the rail is considered. Since the rail form error could be assumed as the periodic function, that is, continuous, the coordinate of pad center can be identified with that of the rail as shown in Fig. 2. Now, the spatial frequency with the wave length λ is defined as $\omega = 2\pi/\lambda$, and the spatial frequency with the wave length l which is equal to the length of pad, is defined as $\omega_l = 2\pi/l$.

Supposing that a pad moves on the rail which has the form error of an arbitrary spatial frequency ω, the variation of film force $f_e(x)$ has the same period with the rail form error. Considering the movement of a multi pad

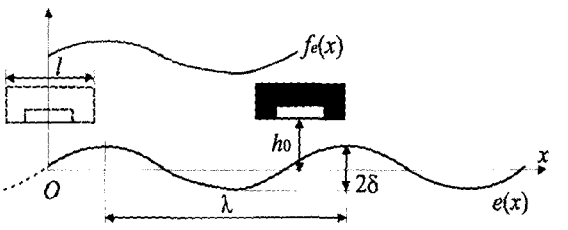

Fig. 2 Response of film force to the sinusoidal profile of the rail

table, the relationship between $f_e(x)$ and the variation of film force in i^{th} pad $f_{ei}(x)$ can be represented as Eq.(6).

$$f_{ei}(x) = f_e(x + X_{ci} - ml/2) \tag{6}$$

Fig. 3 shows the calculated results on the variation of film force, when a pad passes through the one period of rail form error with a single spatial frequency. From the figure, it is confirmed that the variation of film force is approximated to the sinusoidal curve. In calculation, the rail form error is assumed as cosine curve, but in some frequencies such as ω/ω_1=1.5, the profiles of film force are reversed in phase. This aspect mainly occurs by the spatial phase shift between the film force and the rail form error in the land part of the pads. Therefore, if the pocket ratio β is varied, the aspect is changed. On the other hand, in the case of ω/ω_1=2.0 at the lower figure, the variation of film force is very small respectively. This aspect occurs when the pad length approaches to a multiple of the wave length of spatial frequency, and dependent on the pocket ratio. These frequencies are defined as the insensitive frequencies. In reverse, the frequencies at which the film force are largely varied are defined as the sensitive frequencies.

From above, the variation of film force corresponding to a spatial frequency of rail form error can be approximated to sinusoidal curve which has the reverse phase by case. Using this relationship, the transfer function is represented as Eq.(7).

$$K(\omega) = \frac{f_e(\omega)}{e(\omega)} \tag{7}$$

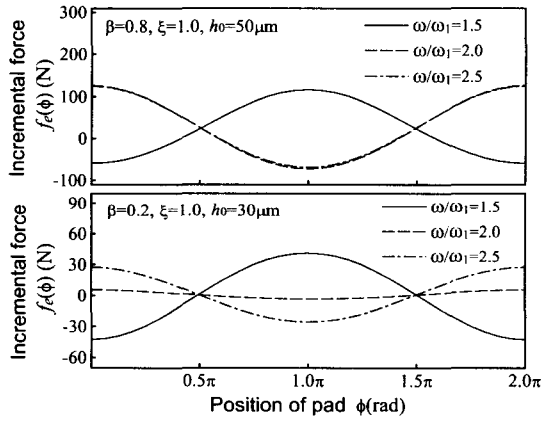

Fig. 3 Increment of the film force caused by the sinusoidal profile of rail

This transfer function also means the averaging effect of an oil film against the spatial frequencies of rail form error in a pad, and its value is reduced when the averaging effect increases. Also, the transfer function at ω = 0 means the static film stiffness of a pad. The transfer function can be obtained by calculating the maximum variation of film force corresponding to a spatial frequency, and by changing the spatial frequency successively from 0 to maximum to be required.

3.2 Calculation of the film force

Using the relations in Eq.(4), (6), (7), and neglecting the periods larger than n + 1, the relationship between the rail form error and the film force is represented as Eq.(8).

$$f_e(x) = \sum_{k=1}^{n} K\left(\frac{2k\pi}{L}\right)\left(a_k \cos\frac{2k\pi}{L}x + b_k \sin\frac{2k\pi}{L}x\right) \tag{8}$$

Supposing that a spatial frequency ω_R has the same wave length with the length of rail L, the relationship between the frequency ω_R based on the length of rail and the frequency ω based on the length of pad is represented as $\omega/\omega_R = (L/l)(\omega/\omega_1)$.

3.3 Analysis of the motion errors

3.3.1 Analysis of a single-side table

The relationship between the linear motion error $z(x)$ and the angular motion error $\theta(x)$ at the table center is as belows;

$$z_i(x) = z(x) + X_{ci}\theta(x)$$
$$X_{ci} = l\{i - (m+1)/2\} \tag{9}$$

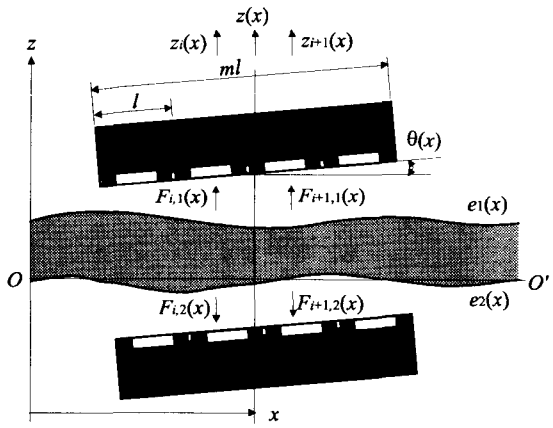

Fig. 4 Static equilibrium of force in a double-sides table

By substituting Eq.(6), (8) and (9) to Eq.(2) and (3), the motion errors are represented as Eq.(10).

$$z(x)=\frac{1}{K_0 m}\sum_{i=1}^{m} f_e(x+X_{ci})$$
$$\theta(x)=\frac{12}{K_0 m(m^2-1)l^2}\sum_{i=1}^{m}\{f_e(x+X_{ci})X_{ci}\} \quad (10)$$

3.3.2 Analysis of a double-sides table

In the case of a double-sides table, the applied load is supported by the difference of film forces in both sides.

Supposing that a double-sides table has the equilibrium state at position x on the rail form errors $e_1(x)$ and $e_2(x)$ as shown in Fig. 4, the equilibrium conditions of force and moment are represented as Eq. (11) and (12). K_{0d} is the static film stiffness of a pad in a double-sides table.

$$\sum_{i=1}^{m}\left[f_{e,1}(x+X_{ci})-f_{e,2}(x+X_{ci})-K_{0d}\{z(x)+X_{ci}\theta(x)\}\right]=0 \quad (11)$$

$$\sum_{i=1}^{m}\left[f_{e,1}(x+X_{ci})-f_{e,2}(x+X_{ci})-K_{0d}\{z(x)+X_{ci}\theta(x)\}\right](X_{ci}+ml/2)=0 \quad (12)$$
$$x=\frac{ml}{2},\cdots,L-\frac{ml}{2}$$

The form errors of the upper and lower rail are represented as Eq.(13).

$$e_1(x)=a_{0,1}+\sum_{k=1}^{\infty}\left(a_{k,1}\cos\frac{2k\pi}{L}x+b_{k,1}\sin\frac{2k\pi}{L}x\right)$$
$$e_2(x)=a_{0,2}+\sum_{k=1}^{\infty}\left(a_{k,2}\cos\frac{2k\pi}{L}x+b_{k,2}\sin\frac{2k\pi}{L}x\right) \quad (13)$$
$$0\le x\le L$$

The linear and angular motion error at the table center derived from Eq.(9) can be represented as Eq.(14), and the variation of film force can be calculated by Eq.(15).

$$z(x)=\frac{1}{K_{0d} m}\sum_{i=1}^{m} f_e(x+X_{ci})$$
$$\theta(x)=\frac{12}{K_{0d} m(m^2-1)l^2}\sum_{i=1}^{m}\{f_e(x+X_{ci})X_{ci}\} \quad (14)$$
$$f_e(x)=f_{e,1}(x)-f_{e,2}(x)$$

$$f_e(x)=\sum_{k=1}^{n}K_d\left(\frac{2k\pi}{L}\right)\left\{(a_{k,1}-a_{k,2})\cos\frac{2k\pi}{L}x+(b_{k,1}-b_{k,2})\sin\frac{2k\pi}{L}x\right\} \quad (15)$$

$K_d(\omega)$ is the transfer function of a double-sides table, which can be calculated by Eq.(7). In this case, $f_e(x)$ is the difference of film forces in both sides pads, which is defined in Eq.(14). The transfer function of a double-sides table can be obtained using the linear characteristics of stiffness as shown in Eq.(16), when the transfer funtion of a single-sides table is already known.

$$K_d(\omega)=\frac{K_{0d}}{K_0}K(\omega) \quad (16)$$

Fig. 5 shows a schematic diagram of motion error analysis algorithm with the transfer function. Comparing with the MPM , the number of mesh is reduced to $1/m$, and iterative process time, which takes most of time for the calculation of attutude, is omitted. Also, the TFM has the merit that it is not necessary to re-calculate the corresponding transfer function once more, even if the rail form error is changed by re-machining or the designed clearance is changed.

4. Theoretical Verification of the TFM

4.1 Setting up the variables

The transfer function is calculated on the period range of ω/ω_1=0 to 10, and the finite element method is used for calculation[3]. Not to be generated the distorted peaks by the digitized meshes in the simulation of the rail profile, the number of node set to be much more than 10 per one period. In the case of comparing the transfer functions or the motion errors according to the varied table dimension, the film stiffness is always preserved constantly by adjusting the resistance ratio ξ. The motion

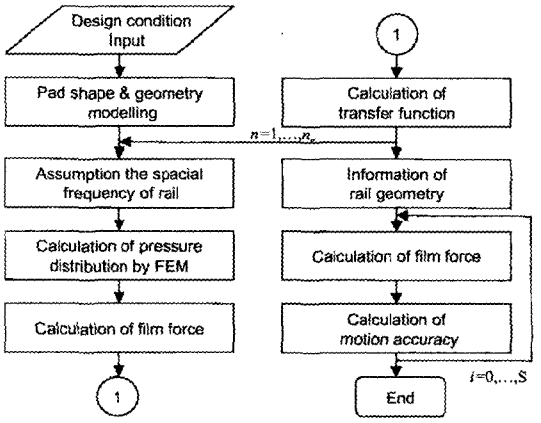

Fig. 5 Flow chart for the analysis of motion errors by the transfer function analysis method

error analysis is carried out on the multi pad type table as shown in Fig. 6. l_s and l_x are assumed to be 0 and 100 mm respectively in the analysis of the transfer function. l_s, l_m and l_x are assumed to be 5, 10 and 90 mm respectively in the motion error analysis.

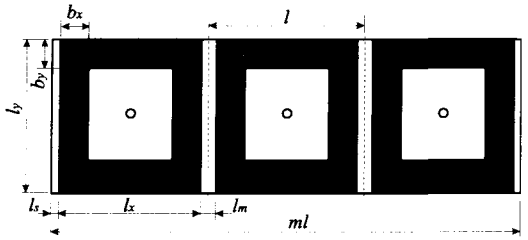

Fig. 6 Parameters on the dimension of hydrostatic tables

4.2 Characteristics of the transfer function

4.2.1 Verification on the sinusoidal approximation

As the variation of film force corresponding to the sinusoidal form error is approximated to sinusoidal curve, it is necessary to examine the calculating error caused by the approximation.

Fig. 7 shows the magnitude and the approximation error of the transfer function when the resistance ratio ξ is 0.2 and 0.8. It is found that the approximation errors are small enough to be neglected.

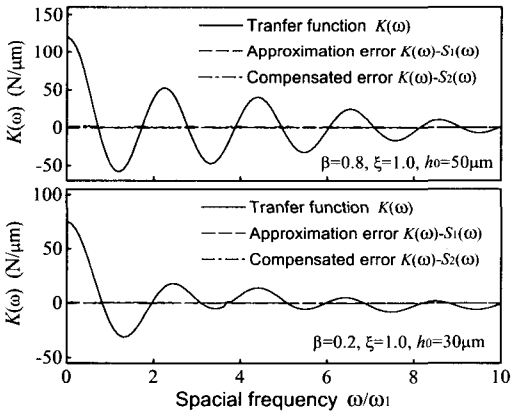

Fig. 7 Approximation error in the calculation of a transfer function

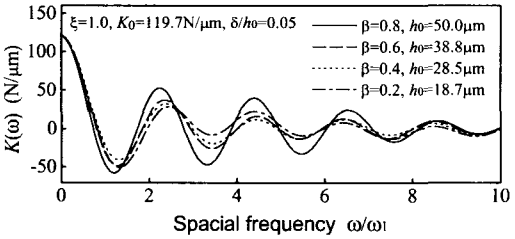

Fig. 8 Influence of the pocket width ratio on the transfer function

4.2.2 Influence of the pad dimension

The relationship between the pocket ratio and the transfer function is shown in Fig. 8. In the calculation, the film stiffness and the resistance ratio are preserved to be constant by adjusting the clearance with the varying pocket ratio.

Comparing the magnitudes of the transfer functions, it is reduced according to the increase of the spatial frequency, and the aspect means that the motion errors become small. In small pocket ratio, the tendency is more obvious. From this result, it is found that the motion errors are improved as the pocket ratio reduces.

The relationship between the pad length and the transfer function is shown in Fig. 9. In the figure, the pocket ratio is preserved to be constant. The magnitude of the transfer function is increased as the pad length increases. But the dimensionless transfer function, which is defined as the ratio of magnitude of the transfer function to the static stiffness, is not changed. Therefore, if the pocket ratio is not changed, the transfer function for the varying pad size can be obtained using the linear characteristics of film stiffness.

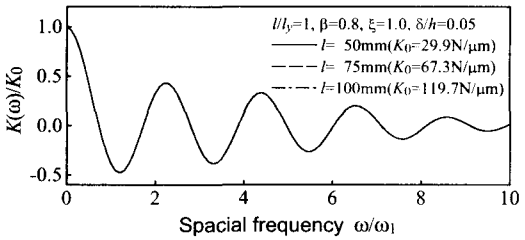

Fig. 9 Relationship between the table dimension and the transfer function

4.2.3 Influence of the magnitude of rail form error

Fig. 10 shows the dimensionless transfer functions according to the varying magitude ratio δ / h_0 of rail form error. The dimensionless transfer functions show good agreement upto $\delta / h_0 = 0.20$. But, at $\delta / h_0 = 0.30$, it shows some difference caused by the nonlinearity between the clearance and the reaction pressure. From this, it is confirmed that the linear relationship between the magnitude of form error and the transfer function can be assumed within the range of $\delta / h_0 <= 0.20$.

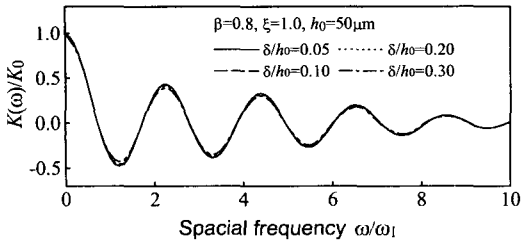

Fig. 10 Relationship between the amplitude of rail form error and the transfer function

4.3 Verification of the motion error analysis method

4.3.1 Case of a single-side table

In order to verify the validity of the TFM, the analyzed results by the TFM are compared with the results by the MPM. The frequency components of an assumed rail for the verification are shown in Fig. 11, and the transfer function of an assumed table is shown in Fig. 12.

Fig. 13(a), (b) shows the analyzed motion errors in the pocket ratio 0.8 and 0.6. In this analysis, the clearance is adjusted to 67 and 52μm in order to preserve the film stiffness to be constant. The analyzed results by both methods show good agreement in all cases.

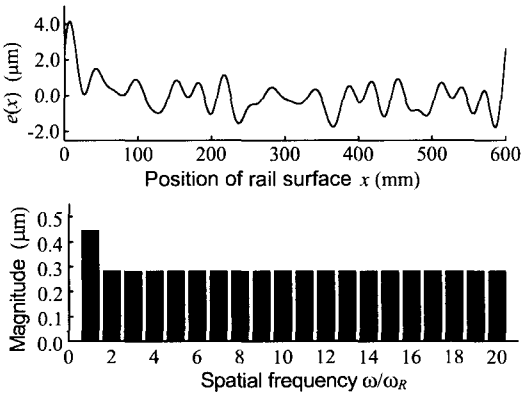

Fig. 11 Rail form error and its frequency components assumed for the simulation of a single-side table

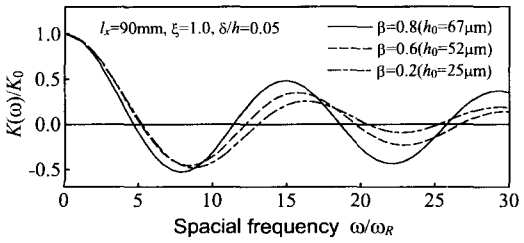

Fig. 12 Transfer function of the analyzed tables

Comparing motion errors, as the pocket ratio reduces, the motion errors are improved quantitatively. Comparing the calculated profiles by both methods, the linear motion errors show good agreement, but angular motion errors show a little difference when the pocket ratio is 0.6 It is seems that the changes of center of moment, inside the pads, are not considered. But, since the difference is quantitatively small enough, it is confirmed that the TFM is very effective to analyze the motion errors of a single-side hydrostatic table.

4.3.2 Case of a double-sides table

The assumed profiles of the upper and lower rail for the analysis of a double-sides table are shown in Fig. 14(a) and (b), and the difference of both rails, which is actually used to the analysis[2], is shown in Fig. 14(c).

Fig. 15(a) and (b) are the analyzed motion errors in the pocket ratio 0.8 and 0.6. The analyzed results by both methods show good agreement. But, the profiles in the pocket ratio 0.6 have a small difference. It is caused by the neglected moment changes inside the pads, as well as

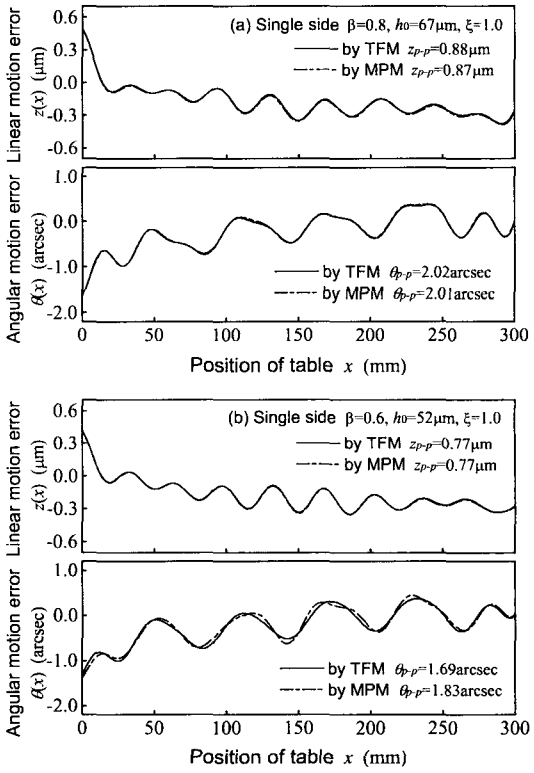

Fig. 13 Analyzed motion errors with the varying pocket ratio in a single-side table

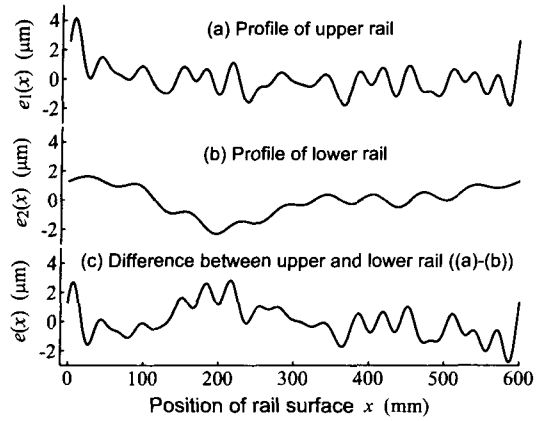

Fig. 14 Rail form errors assumed for the simulation of a double-sides table

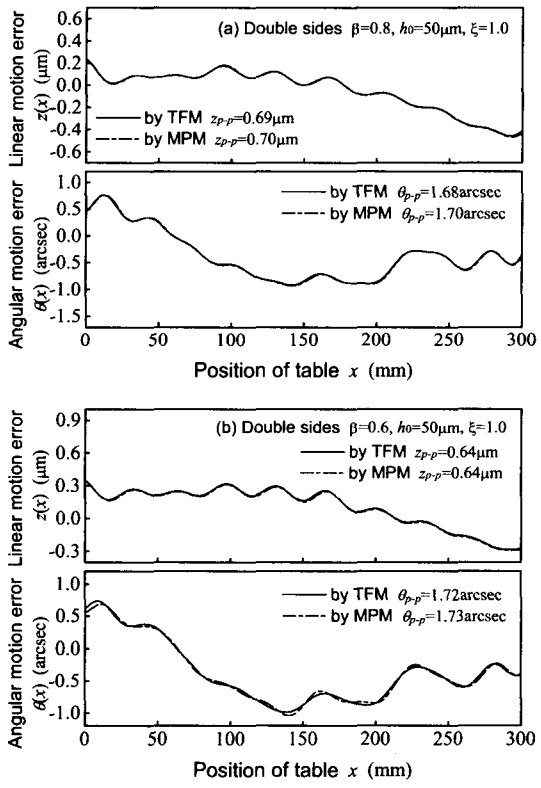

Fig. 15 Analyzed motion errors with the varying pocket ratio in a double-sides table

the case of a single-side table.

From the comparison of motion errors by both methods in a single-side table and a double-sides table, it is confirmed that the analyzed results show good agreement and therefore, the TFM is very effective to analyze the motion errors of hydrostatic tables.

5. Conclusions

In this paper, the motion error analysis method of hydrostatic tables using a transfer function is proposed and verified theoretically. The obtained results are as follows;

1) The analyzed results by the TFM show good agreement with the results by the proven MPM. Therefore it is confirmed that the TFM is an effective method to analyze the motion errors.
2) The transfer function introduced in this paper clarifies quantitatively the averaging effect of an oil film in a hydrostatic pad.
3) Basically, the averaging effect of an oil film is increased relatively, as the frequency component of rail form error is higher. Also, the insensitive frequencies of rail form error, which occur when the pad length is approximately a multiple of the wave length of the frequencies, have no effect on the motion errors.
4) As the dimensionless transfer function is not affected by the pad dimension but by the pocket ratio, the variation of design variables such as the clearance and the supplied oil pressure, has no effect on the motion errors.

Acknowledgement

The authors gratefully acknowledge the support of Ministry of Science and Technology under the National Research Laboratory project.

References

1. Park, C. H., Chung, J. H., Lee, H. and Kim, S. T., "Finite Element Analysis on the Motion Accuracy of Hydrostatic Table (1st. Analysis and Experimental Verification on Single-side Table)," Jr. of KSPE, Vol. 17, No. 12, pp. 137-144, 2000.
2. Park, C. H., Lee, H., Kim, T. H. and Kim, M. G., "Finite Element Analysis on the Motion Accuracy of Hydrostatic Table (2nd. Analysis and Experimental Verification on Double-sides Table)," Jr. of KSPE, Vol. 19, No. 1, pp. 65-70, 2002.
3. Aoyama, T., "Hydrostatic Bearing - Design and Applications -," Kougyojoushakai, 1990.